World Journal of Gastroenterology

Online Submissions: http://www.wjgnet.com/1007-9327office
wjg@wjgnet.com
doi:10.3748/wjg.v17.i43.4757

World J Gastroenterol 2011 November 21; 17(43): 4757-4771
ISSN 1007-9327 (print) ISSN 2219-2840 (online)

REVIEW

Spectrum of mucin-producing neoplastic conditions of the abdomen and pelvis: Cross-sectional imaging evaluation

Nam Kyung Lee, Suk Kim, Hyun Sung Kim, Tae Yong Jeon, Gwang Ha Kim, Dong Uk Kim, Do Youn Park, Tae Un Kim, Dae Hwan Kang

Nam Kyung Lee, Suk Kim, Department of Radiology, Pusan National University Hospital and Medical Research Institute, Pusan National University School of Medicine, Pusan National University, Busan 602-739, South Korea
Hyun Sung Kim, Tae Yong Jeon, Department of Surgery, Pusan National University Hospital and Medical Research Institute, Pusan National University School of Medicine, Pusan National University, Busan 602-739, South Korea
Gwang Ha Kim, Dong Uk Kim, Department of Internal Medicine, Pusan National University Hospital and Medical Research Institute, Pusan National University School of Medicine, Pusan National University, Busan 602-739, South Korea
Do Youn Park, Department of Pathology, Pusan National University Hospital and Medical Research Institute, Pusan National University School of Medicine, Pusan National University, Busan 602-739, South Korea
Tae Un Kim, Department of Radiology, Yangsan Pusan National University Hospital and Medical Research Institute, Pusan National University School of Medicine, Pusan National University, Yangsan 626-770, South Korea
Dae Hwan Kang, Department of Internal Medicine, Yangsan Pusan National University Hospital and Medical Research Institute, Pusan National University School of Medicine, Pusan National University, Yangsan 626-770, South Korea
Author contributions: Kim S contributed to study conception and design; Lee NK, Kim HS, Jeon TY, Kim GH, Kim DU, Park DY, Kim TU, and Kang DH contributed to acquisition of data, or analysis and interpretation of data; Lee NK and Kim S contributed to drafting the article or revising it critically for important intellectual content; Kim S gave final approval of the version to be published.
Supported by A grant from the Korea Healthcare Technology R and D Project, Ministry for Health, Welfare, and Family Affairs, South Korea, A091047
Correspondence to: Suk Kim, MD, Department of Radiology, Pusan National University Hospital and Medical Research Institute, Pusan National University School of Medicine, Pusan National University, No. 1-10, Ami-Dong, Seo-Gu, Busan 602-739, South Korea. kimsuk@medimail.co.kr
Telephone: +82-51-2407354 Fax: +82-51-2447534
Received: February 23, 2011 Revised: March 29, 2011
Accepted: April 5, 2011
Published online: November 21, 2011

Abstract

Various mucin-producing neoplasms originate in different abdominal and pelvic organs. Mucinous neoplasms differ from non-mucinous neoplasms because of the differences in clinical outcome and imaging appearance. Mucinous carcinoma, in which at least 50% of the tumor is composed of large pools of extracellular mucin and columns of malignant cells, is associated with a worse prognosis. Signet ring cell carcinoma is characterized by large intracytoplasmic mucin vacuoles that expand in the malignant cells with the nucleus displaced to the periphery. Its prognosis is also generally poor. In contrast, intraductal papillary mucinous neoplasm of the bile duct and pancreas, which is characterized by proliferation of ductal epithelium and variable mucin production, has a better prognosis than other malignancies in the pancreaticobiliary tree. Imaging modalities play a critical role in differentiating mucinous from non-mucinous neoplasms. Due to high water content, mucin has a similar appearance to water on ultrasound (US), computed tomography (CT), and magnetic resonance imaging, except when thick and proteinaceous, and then it tends to be hypoechoic with fine internal echoes or have complex echogenicity on US, hyperdense on CT, and hyperintense on T1- and hypointense on T2-weighted images, compared to water. Therefore, knowledge of characteristic mucin imaging features is helpful to diagnose various mucin-producing neoplastic conditions and to facilitate appropriate treatment.

Key words: Mucin; Neoplasm; Ultrasound; Computed tomography; Magnetic resonance; Abdomen and pelvis

Peer reviewer: Edward J Ciaccio, PhD, Research Scientist, Department of Medicine, HP 804, Columbia University, 180 Fort Washington Avenue, New York, NY 10032, United States

Lee NK, Kim S, Kim HS, Jeon TY, Kim GH, Kim DU, Park DY, Kim TU, Kang DH. Spectrum of mucin-producing neoplastic conditions of the abdomen and pelvis: Cross-sectional imaging evaluation. *World J Gastroenterol* 2011; 17(43): 4757-4771 Available from: URL: http://www.wjgnet.com/1007-9327/full/v17/i43/4757.htm DOI: http://dx.doi.org/10.3748/wjg.v17.i43.4757

INTRODUCTION

Mucinous carcinoma is a histological subtype of tumor in which at least 50% of the tumor is composed of large pools of extracellular mucin and columns of malignant cells. Although less frequent than non-mucinous carcinoma, mucinous carcinoma is associated with a worse prognosis, because it is more frequently diagnosed in the advanced stage and is associated with more frequent local recurrence, serosal invasion, lymphatic and vascular invasion, lymph node metastasis, and distant metastasis[1,2]. Signet ring cell carcinoma is composed of signet ring cells that have a vacuolated cytoplasm containing abundant intracellular mucin and a nucleus displaced to the periphery. The prognosis for signet ring cell carcinoma is generally poor, although its prognosis is still controversial[3,4]. Intraductal papillary mucinous neoplasm (IPMN) is an uncommon neoplasm arising from the bile duct and pancreas, which is characterized by a proliferation of ductal epithelium associated with ductal dilatation and variable mucin production. Distinguishing IPMN from other tumors is essential because IPMN has a better prognosis than other malignancies in the pancreaticobiliary tree[5,6].

Careful distinction of mucinous and non-mucinous tumors is important, as the clinical outcome of these entities may somewhat differ. Because abundant mucin within the tumor is the hallmark of mucinous neoplasms, mucin-producing neoplasms typically show some distinct imaging features. Therefore, familiarity with the critical imaging features of mucin-producing neoplasms in the abdomen and pelvis may facilitate an accurate diagnosis and treatment.

In this article, we classify mucin-producing neoplasms in the abdomen and pelvis into four types according to characteristic morphological features: unilocular or multilocular cystic neoplasms lining mucin-secreting epithelium that contain mucinous fluid; tumors characterized by intraluminal proliferation of mucinous neoplastic transformation of epithelium lining pancreaticobiliary ducts, which are arranged in a papillary pattern and typically produce and accumulate mucin; tumors composed of neoplastic epithelium containing intracellular mucin associated with little or no extracellular mucin; and tumors composed of abundant extracellular mucin due to mucin-secreting neoplastic epithelium. On the basis of these four types, we discuss and illustrate the clinical significance and imaging features of mucin-producing neoplasms in the abdomen and pelvis.

BASIC CONCEPTS

Mucin is a high-molecular-weight glycoprotein containing oligosaccharides attached to the mucin core protein, and is the major component of mucus lining the surface of glandular epithelium as a viscoelastic gel. Mucin is expressed by various epithelial mucosal cells, which exist in the respiratory, digestive, and urogenital tracts, and secretory epithelial surfaces of specialized organs such as the liver, pancreas, gallbladder, kidneys, salivary glands, lacrimal glands, and eyes. Mucin has a central role in maintaining homeostasis and promoting cell survival in a variety of conditions. Because the outermost area of a typical epithelial surface consists of secreted gel-forming mucin, mucin lubricates and forms a barrier that protects the mucosal epithelium from potentially noxious intraluminal substances such as air, food, enzymes, acidic pH, salt, bacteria, and viruses. Additionally, mucin gels capture and hold biologically active molecules that may incite inflammatory, repair, or healing processes following their release[7,8].

Cancer cells, especially adenocarcinomas, express aberrant forms or amounts of mucins that arise as a consequence of the deregulation of mucin core protein expression. Mucins in cancer cells contribute to carcinogenesis and tumor invasion by simultaneously disrupting existing interactions and establishing new ones. These tumors produce variable amounts of intracellular and/or extracellular mucins[9].

Mucus is composed of 95% water and 5% high-molecular-weight glycoprotein. Due to its high water content, mucin usually appears anechoic on ultrasound (US), and has computed tomography (CT) attenuation and magnetic resonance (MR) signal intensity similar to those of water. However, the imaging appearance of mucin varies depending on water and protein concentrations. Concentrated mucin increases US echogenicity, which may appear hypoechoic with fine internal echoes or in a complex echogenic pattern. Concentrated mucin also has CT attenuation values above that of water, as well as high signal intensity on T1-weighted images and low signal intensity on T2-weighted images due to shortening of both the T1 and T2 relaxation times[10]. Knowledge of these characteristic mucin imaging features is helpful to diagnose various mucin-producing neoplastic conditions and to avoid pitfalls.

MUCIN-PRODUCING NEOPLASTIC CONDITIONS

Well-circumscribed cystic neoplasms lining mucin-secreting epithelium and containing mucinous fluid

Mucinous cystic neoplasm of the pancreas: A mucinous cystic neoplasm (MCN) is lined by mucin-producing columnar epithelium. This tumor is characterized by an ovarian-like stromal component, which is essential for diagnosing MCN of the pancreas. MCN of the pancreas

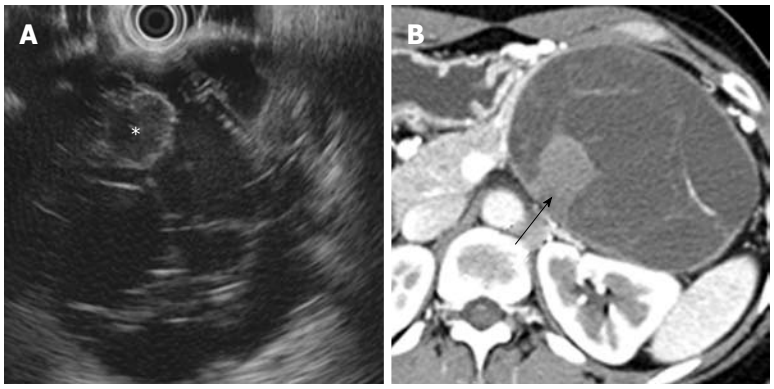

Figure 1 Mucinous cystadenoma of the pancreas in a 40-year-old woman. A: Endoscopic ultrasound image shows a complex multiloculated cystic mass in the pancreatic tail. Note a hyperechoic locule (asterisk) within the cystic tumor; B: Contrast-enhanced CT image shows a well-circumscribed multiloculated mass in the tail of the pancreas with enhancement of thin internal septa and the peripheral wall. Note a highly attenuated locule (arrow) within the cystic tumor. CT: Computed tomography.

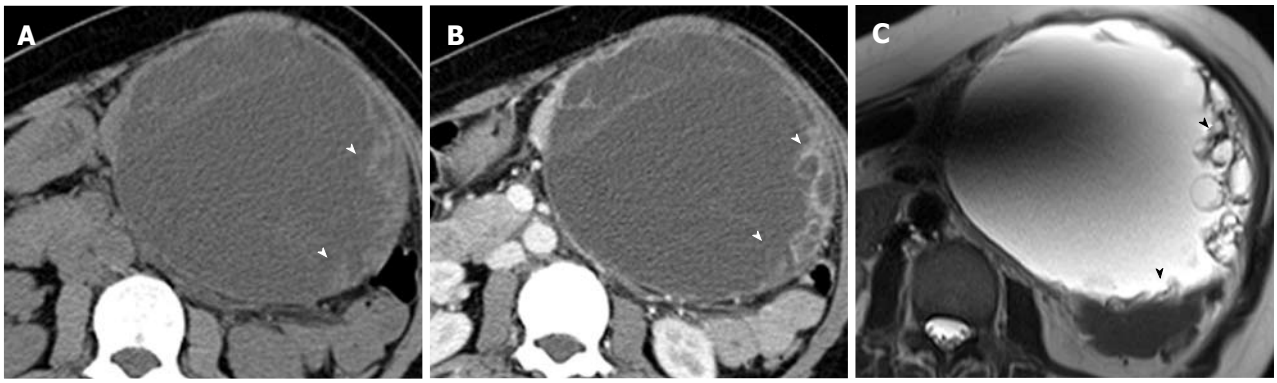

Figure 2 Mucinous cystadenocarcinoma of the pancreas in a 44-year-old woman. A, B: Non-enhanced (A) and contrast-enhanced (B) CT images show a well-circumscribed multi-septated cystic mass with enhancing soft tissue components (arrowheads) in the tail of the pancreas; C: T2-weighted MR image shows a large multilocular cystic mass with high signal intensity and peripheral soft tissue components with low signal intensity (arrowheads) in the pancreatic tail. CT: Computed tomography; MR: Magnetic resonance.

shares both clinical and pathological characteristics with biliary and ovarian mucinous tumors[11]. MCN occurs predominantly in middle-aged women, typically in the body or tail of the pancreas. Although a spectrum of MCNs from benign (mucinous cystadenoma) to malignant (mucinous cystadenocarcinoma) occurs, MCNs should always be resected because they are all potentially malignant[11].

On cross-sectional imaging, a MCN appears as a well-capsulated, unilocular, or multilocular septated cystic lesion (Figures 1 and 2). The tumor is round to oval with a smooth external margin, and the wall of the cyst is typically thick with delayed enhancement[11,12]. Peripheral calcification is seen in 10%-25% of cases and is an important characteristic of MCN that can be used to distinguish it from serous cystadenoma, which tends to have central calcification[11]. A MCN generally does not communicate with the pancreatic duct, unlike an IPMN-P. When rarely present, such a communication is due to fistula formation between the MCN and the pancreatic duct[13]. Different attenuations or signal intensities may be noted within the cystic cavity, depending on whether mucoid or hemorrhagic fluid is present. The presence of an internal enhancing soft tissue component is indicative of mucinous cystadenocarcinoma (Figure 2)[11,14].

Biliary cystadenoma and cystadenocarcinoma: Biliary cystadenomas and cystadenocarcinomas are rare tumors arising in the bile duct epithelium as multilocular cystic masses containing carcinoembryonic antigen-rich mucinous fluid. They are generally intrahepatic (85%) and occur more frequently in middle-aged women. These tumors are similar to mucinous cystic tumors that arise in the pancreas and ovary and are further subdivided into those with ovarian stroma and those without ovarian stroma. The presence of ovarian stroma may be a favorable prognostic sign. However, gross or imaging features cannot distinguish tumors with ovarian stroma from those without ovarian stroma[15,16].

The CT appearance of a biliary cystadenoma and cystadenocarcinoma includes a solitary cystic mass with a well-defined thick fibrous capsule, mural nodules, internal septa, and, rarely, capsular calcification. These appear as a multilocular cystic mass with variable signal intensities on both T1- and T2-weighted images depending on the

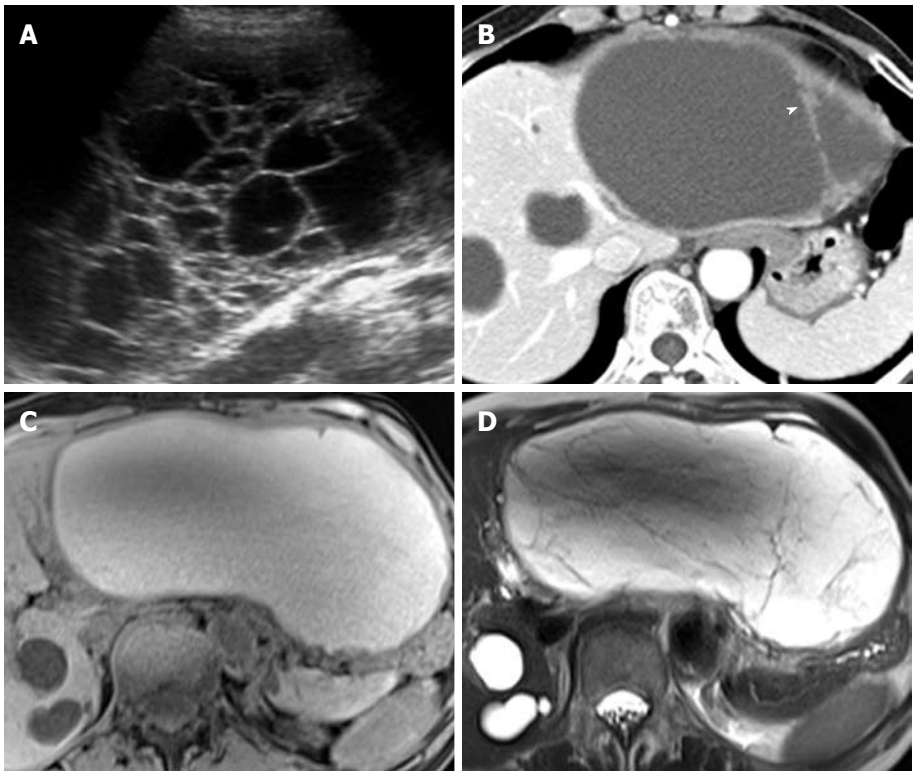

Figure 3 Biliary cystadenoma in the liver of a 55-year-old woman. A: Ultrasound image shows a multiseptated cystic mass in the liver; B: Contrast-enhanced CT image shows a well-circumscribed cystic liver mass, which has similar attenuation to that of hepatic cysts. Note the internal septa with nodular thickening (arrowhead); C, D: T1- (C) and T2-weighted (D) MR images show a multiseptated cystic mass with hyperintensity. CT: Computed tomography; MR: Magnetic resonance.

presence of mucin, hemorrhage content, or solid components (Figure 3)[17]. Internal nodularity and septation have been associated with a biliary cystadenocarcinoma, whereas septation without nodularity is associated with a biliary cystadenoma. However, these findings overlap between benign and malignant forms. Because both a biliary cystadenoma and cystadenocarcinoma are treated with total surgical excision, distinguishing these two diseases may be of little practical importance[15,16].

Biliary cystadenomas and cystadenocarcinomas morphologically resemble a cystic variant of an intrahepatic intraductal papillary neoplasm of the bile duct (IPN-B). Distinguishing these two diseases may be possible on images in which the cystic IPN-B is communicating with the intrahepatic bile ducts and the downstream bile duct is dilated due to excessive mucin, whereas biliary cystadenomas and cystadenocarcinomas do not communicate with the bile duct, and mucin is confined to the cystic mass[18].

Mucinous cystic tumors of the ovary: Mucinous cystic tumors of the ovary are the second most common type of ovarian epithelial tumor. They can be classified as adenomas, borderline malignancies, or adenocarcinomas, according to the histopathological degree of malignancy. A mucinous cystadenoma is composed of a single layer of columnar cells with abundant intracellular mucin and small basilar nuclei in the cysts. A mucinous borderline tumor is a noninvasive epithelial tumor characterized by cytologic atypia without stromal invasion. A mucinous cystadenocarcinoma has an irregular glandular structure and papillae with obvious stromal invasion[19].

On MR imaging, a mucinous cystic tumor typically appears as a large multilocular cystic mass. The loculi show variable signal intensity on both T1- and T2-weighted images (so-called "stained glass" appearance), depending on the viscosity of the materials present, such as mucin, blood products, or debris (Figures 4, 5 and 6). A unilocular cystic appearance is rare for mucinous cystic tumors. A solid component, thick septa, and a thick and irregular wall are suggestive of a malignant epithelial ovarian tumor (Figure 6)[20,21].

A primary intestinal mucinous carcinoma, most commonly from the appendix or colon, can metastasize to the ovary. Metastases to ovary are much more common than an ovarian cystadenocarcinoma. A metastatic carcinoma is often bilateral, whereas a mucinous cystadenocarcinoma is usually unilateral. However, mucinous cystadenocarcinomas mimic metastases to the ovary from a primary mucinous carcinoma on MR imaging[20,21].

The gross and radiological appearances of mucinous borderline tumors usually do not reliably distinguish them from cystadenomas or even some cystadenocarcinomas. The most frequent MR feature of mucinous borderline tumors is a predominantly cystic lesion with varying cyst and septal wall thickness. Mucinous borderline tumors and cystadenocarcinomas tend to have greater numbers of loculi on MR imaging than cystadenomas, which can be explained by more active mitosis in mucinous bor-

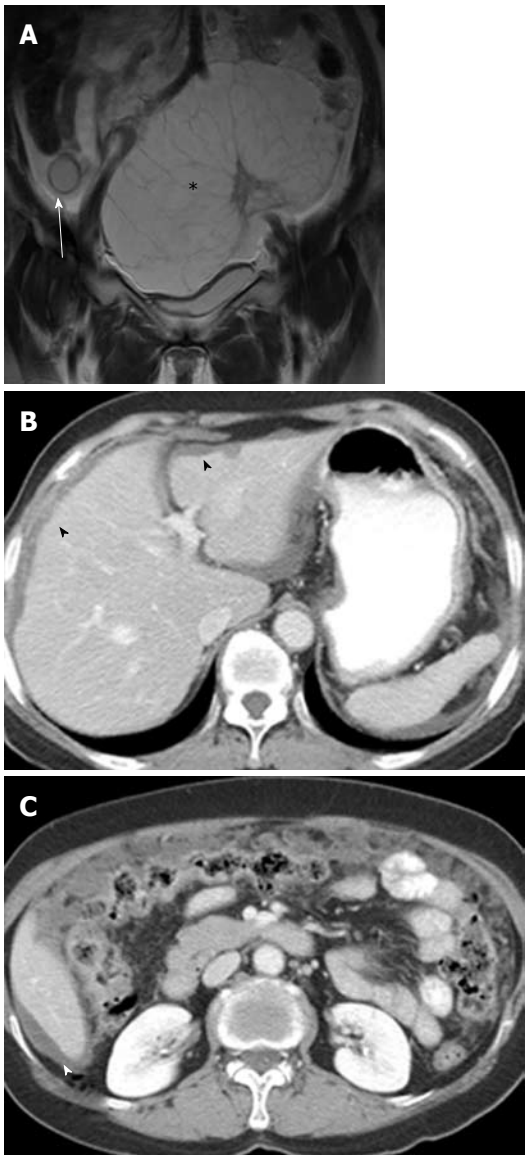

Figure 4 Coexistence of a mucinous cystadenoma of the appendix and ovary in a 63-year-old woman. A: Coronal T2-weighted MR image shows a well-defined cystic mass with hyperintensity in the appendix (arrow) and a multiloculated cystic mass in the left ovary (asterisk); B, C: Contrast-enhanced CT images show low-attenuation mucinous deposits in the peritoneal cavity and scalloping of the liver margin (arrowheads), suggestive of pseudomyxoma peritonei. CT: Computed tomography; MR: Magnetic resonance.

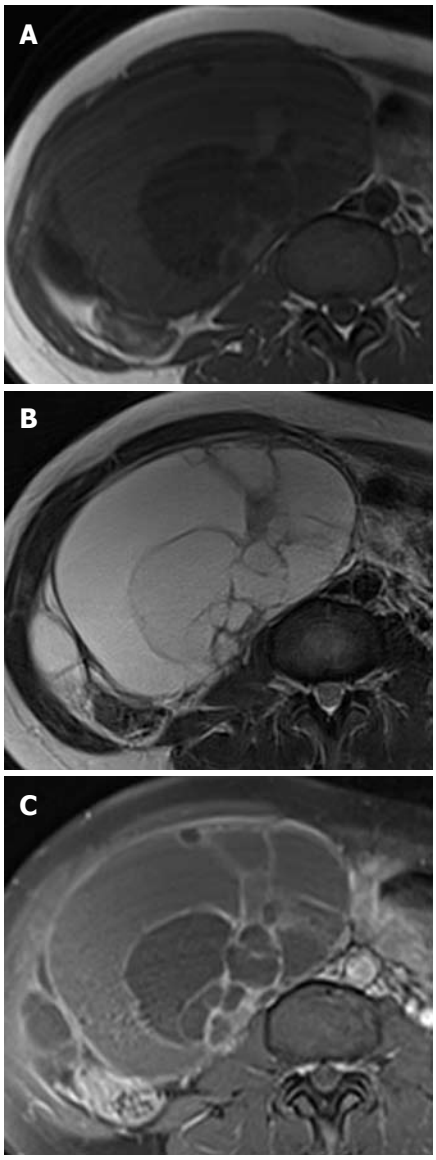

Figure 5 Mucinous borderline tumor of the right ovary in a 41-year-old woman. A, B: T1- (A) and T2-weighted (B) MR images show a cystic mass with large numbers of loculi with varying signal intensity in the right ovary; C: Contrast-enhanced fat-saturated T1-weighted MR image shows the enhancement of multiple internal septa and wall in the cystic mass. MR: Magnetic resonance.

derline tumors and cystadenocarcinomas, resulting in production of larger numbers of glands and loculi (Figures 5 and 6). Both mucinous cystadenocarcinomas and borderline tumors show a solid portion on MR imaging, which is pathologically composed of densely aggregated fine numerous loculi or diffuse tumor cell proliferation. However, the solid portion of a mucinous cystadenocarcinoma is larger and more commonly seen than in a borderline tumor. Pelvic organ invasion, implants, and lymphadenopathy may be helpful ancillary findings suggestive of malignancy[22,23].

Mucocele of the appendix: Mucocele is a descriptive term for a mucinous distension of the appendiceal lumen, regardless of the underlying pathology. A mucocele is quite rare, with a prevalence of 0.2%-0.3% among appendectomies and 8% of all appendiceal tumors. A mucocele can be caused by a variety of nonneoplastic, benign neoplastic, and malignant conditions. However, most mucoceles are associated with neoplastic epithelium. A mucinous cystadenoma is the most common type, representing 63%-84% of mucoceles. A mucinous cystadenoma is based on villous adenomatous changes in the mucin-rich epithelium, which produce marked intraluminal dilatation by mucin reaching up to 6 cm. An appendiceal perforation occurs in up to 20% of cases, with mucinous spillage into the periappendiceal area or onto the serosal surface, which leads to pseudomyxoma

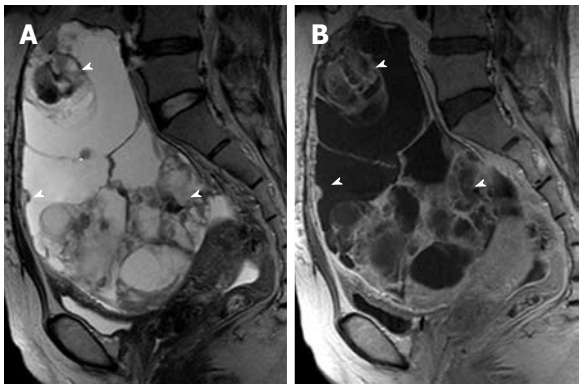

Figure 6 Mucinous cystadenocarcinoma of the left ovary in a 47-year-old woman. A: Sagittal T2-weighted MR image shows a huge multilocular ovarian cystic mass with multiple hypointense solid components (arrowheads); B: Sagittal contrast-enhanced T1-weighted MR image shows an ovarian cystic mass with enhancement of internal septa and solid components (arrowheads). MR: Magnetic resonance.

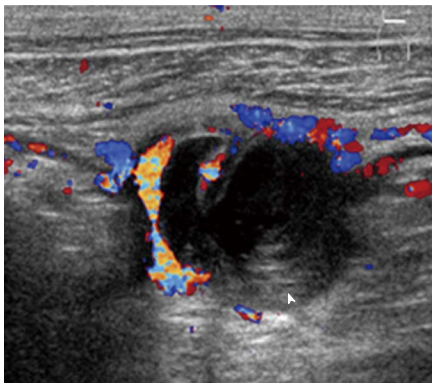

Figure 7 Mucocele of the appendix in a 54-year-old man. Ultrasound image shows an anechoic round mass in the appendix with echogenic layers (arrowhead) (the so-called "onion-skin" sign).

peritonei (PMP) and a possibly fatal outcome. A mucinous cystadenocarcinoma is less common than a cystadenoma, accounting for 11%-20% of cases. The presence of stromal invasion by neoplastic cells is indicative of an adenocarcinoma[24,25].

Imaging plays an important role when evaluating appendiceal mucocele. US usually reveals a unilocular, ovoid, anechoic mass in the region of the appendix. Internal echogenicity varies depending on the acoustic interfaces produced by the mucin, including hypoechoic masses with fine internal echoes and complex echogenic masses with acoustic enhancement. Concentric and echogenic layers within the cystic mass (the so-called "onion skin" sign) are specific for mucocele of the appendix (Figure 7). The reason for the layered appearance on US is unclear; nevertheless, it may be explained by a fluctuation in mucin secretion into the cavity along with the gradual absorption of water or by a fluctuation in the degree of excretion blockage from the cavity[24,26]. CT is the imaging modality of choice because CT depicts tissue characteristics, the anatomical relationship between the cystic mass

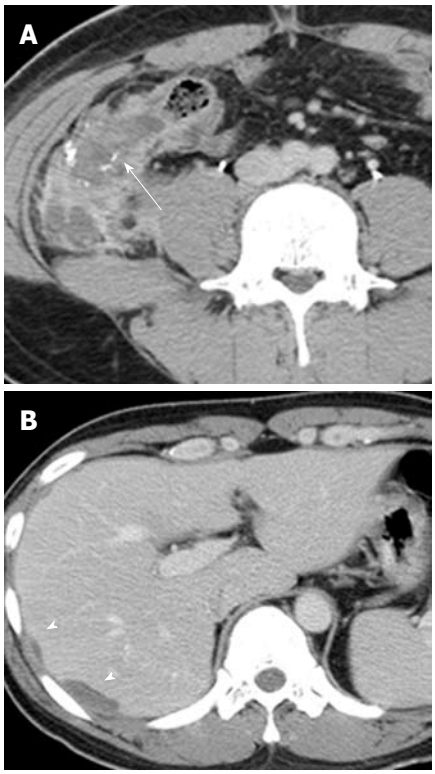

Figure 8 Mucinous cystadenocarcinoma of the appendix in a 26-year-old man. A: Contrast-enhanced CT image shows a complex hypoattenuating mass with enhancing solid portions and punctate calcifications in the appendix (arrow); B: Contrast-enhanced CT image of the upper abdomen shows loculations of fluid scalloping on the liver surface (arrowheads), providing evidence of a mass effect. CT: Computed tomography.

and cecum, and helps rule out or confirm the diagnosis. On CT, a mucocele appears as a round or tubular cystic mass with thin and enhancing walls, which is contiguous with the base of the cecum. Curvilinear mural calcification is sometimes seen in less than 50% of cases, which is suggestive of a mucocele. A mucocele is hyperintense on T2-weighted image and variably hypointense or isointense on T1-weighted image, depending on the mucin concentration (Figure 4). The presence of enhancing nodular lesions raises the possibility of a mucinous cystadenocarcinoma (Figure 8). Identifying a normal right ovary in women is also crucial to exclude a cystic ovarian neoplasm or tubo-ovarian abscess[24,25,27].

Since mucoceles usually present as a chronic noninfectious process, most are relatively asymptomatic. However, their presenting symptoms sometimes mimic acute appendicitis. The differential diagnosis between a mucocele with secondary appendicitis and appendicitis without a mucocele is important because surgical management may be altered according to the presence or absence of mucocele. CT features such as cystic dilatation of the appendix, a luminal diameter greater than 1.5 cm, and mural calcification suggest a mucocele coexisting with acute appendicitis, although there is some overlap with the diagnosis of acute appendicitis without a mucocele[28].

The treatment of choice is surgical excision, and the

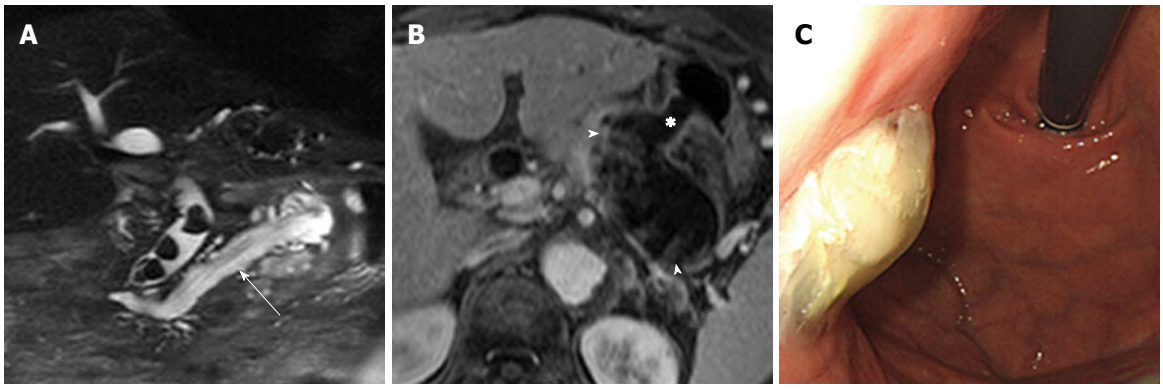

Figure 9 Intraductal papillary mucinous neoplasm of the pancreas in an 80-year-old woman. A: Coronal T2-weighted RARE MR image shows cord-like hypointense mucin in the dilated main pancreatic duct (arrow). Note multiple stones in the dilated common bile duct; B: Axial contrast-enhanced fat-saturated T1-weighted MR image demonstrates a fistula (asterisk) between the dilated main pancreatic duct and the stomach. Note mural nodules (arrowheads) within the dilated main pancreatic duct, which strongly suggest a malignant Intraductal papillary mucinous neoplasm; C: Endoscopy image reveals mucin leaking from the papilla. RARE: True rapid acquisition with relaxation enhancement; MR: Magnetic resonance.

type of surgery performed is related to the size and the histological contents of the mucocele. A full abdominal exploration is advised during surgery, because a mucocele can be associated with other tumors, particularly colonic adenocarcinoma and ovarian tumors[26].

Tumors that produce and accumulate mucin in the pancreaticobiliary tract

Intraductal papillary mucinous neoplasm of the pancreas: IPMN-P, known as one of the mucin-producing pancreatic tumors, is an uncommon pancreatic neoplasm with characteristic histology and distinctive clinicobiological behavior. It is characterized by an intraductal proliferation of mucinous cells arranged in a papillary pattern. Excessive mucin secretion in the ducts by this proliferation ultimately leads to cystic dilatation of the major duct, the second duct, or both, depending on the tumor location. Abundant mucin production is usually observed in most cases of IPMN-P. The clinical symptoms and signs of IPMN-P are due to impaired outflow of pancreatic juice, which is induced by the hypersecretion of mucin[5,29].

IPMN-P occurs most frequently in men, and the mean age at the time of diagnosis is approximately 60 years. It is most commonly located in the head or uncinate process of the pancreas. IPMN-P has a low potential for malignancy, and it has a better prognosis than other pancreatic malignancies because of slow growth rates, rare parenchymal invasion, low rates of metastatic spread, and low recurrence after resection[5,29].

Characteristic endoscopic retrograde cholangiopancreatography findings of IPMN-P include communication between a cystic lesion in the branch duct and the main pancreatic duct, intraluminal filling defects of the pancreatic duct due to the presence of mucin or a mass, and the depiction of a patulous papilla with mucin extrusion from the orifice of the papilla. CT or MR findings of IPMN-P include grapelike clustered cystic lesions reflecting focal dilatation of the branch ducts, diffuse dilatation of the main pancreatic duct, mural nodules, bulging papilla, and communication of branch duct-type IPMN with the main pancreatic duct. Although the diagnosis of malignancy in IPMN is often difficult, even with recent advanced MR techniques, several indirect findings can suggest the presence of malignancy, including the presence of mural nodules, thick septa, septal calcification, and a main pancreatic duct dilated to greater than 10 mm in diameter (Figure 9)[5].

Papillary neoplasm of the bile duct: A papillary neoplasm of the bile duct is an intraductal tumor with numerous minute frondlike papillary projections. In approximately one-third of cases, tumors produce abundant viscous mucin, resulting in intermittent and incomplete obstruction of the segmental or lobar bile ducts or the entire biliary tree. A papillary neoplasm of the bile ducts arises from the mucosa and slowly spreads along its luminal surface. Only in the late stage does it invade the bile duct, and thus prognosis is relatively favorable[6,30].

Considering the shared biliary tract and pancreatic origin, the two systems may have similar pathological features. Thus, IPN-B is the biliary counterpart of IPMN-P. In both organs, these neoplasms arise within the duct system and show a predominantly intraductal growth pattern, commonly an overproduction of mucin, and an association with invasive adenocarcinoma[30].

Based on the gross appearance of the intraductal tumors, IPN-B may be classified as an intraductal polypoid tumor, a cast-like growing tumor, a mucosal spreading growth, a cystic variant, or a floating tumor[31]. Thus, variable imaging appearances of IPN-B include an intraductal polypoid mass within a localized ductal dilatation, diffuse and marked duct ectasia with a visibly enhanced papillary mass or masses, intraductal cast-like lesions within a mildly dilated duct, diffuse and marked duct ectasia without a visible mass, or a floating tumor. The friable part of the papillary tumor may slough off and be seen in imaging as a floating tumor within the bile duct, which can be radiologically confused with a bile duct stone[32,33].

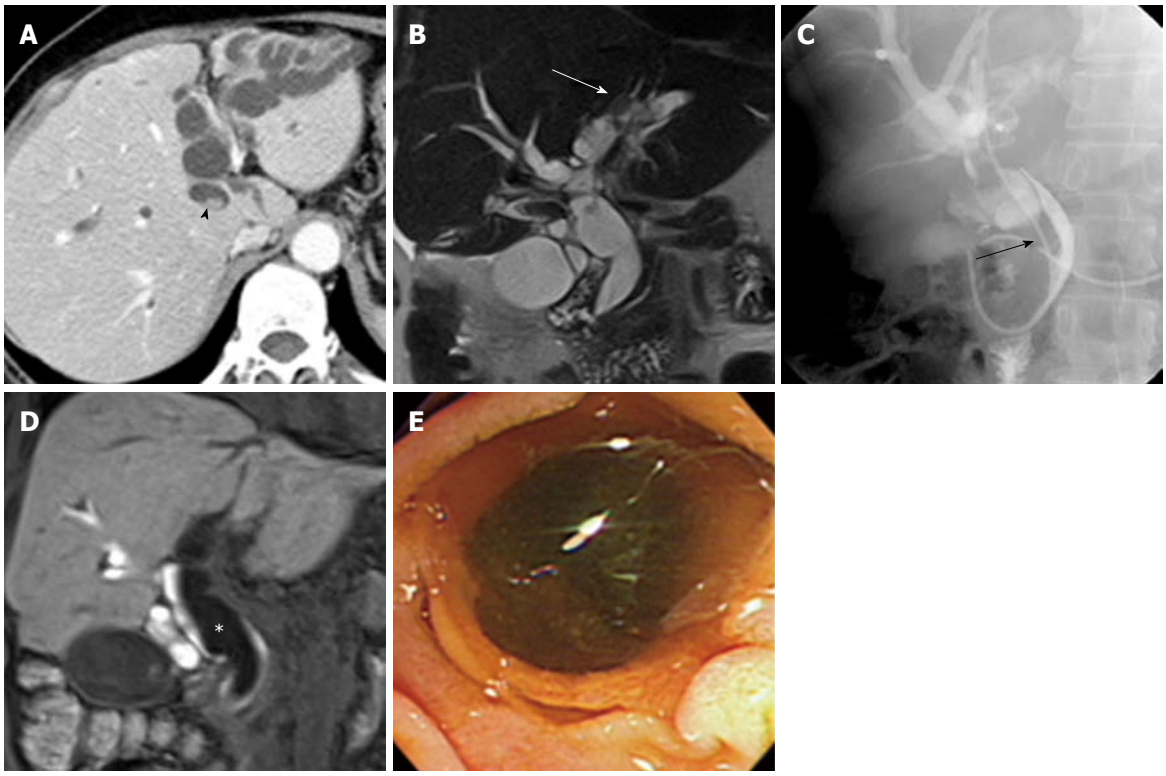

Figure 10 Intraductal papillary mucinous neoplasm of the bile duct in a 58-year-old woman. A: Contrast-enhanced CT image shows severe dilatation of the left intrahepatic ducts without visible intraductal mass. Note a small stone in the dilated intrahepatic duct (arrowhead); B: Coronal T2-weighted RARE MR image shows dilatation of the intrahepatic and extrahepatic ducts. Note the hypointense intraductal mass (arrow) in the left intrahepatic duct; C: Endoscopic retrograde cholangiogram image shows a filling defect (arrow) within the marked dilated extrahepatic bile duct, due to mucin; D: Coronal gadoxetic acid-enhanced T1-weighted MR image obtained at 60 min post-injection shows contrast-filled bile duct with an elongated, low signal intensity lesion (asterisk), which represents mucin; E: Endoscopy image reveals mucin leaking from the papilla. CT: Computed tomography; RARE: True rapid acquisition with relaxation enhancement; MR: Magnetic resonance.

CT and MR images may fail to detect mucin itself because the attenuation or signal intensity of mucin is usually similar to that of bile. A large amount of mucin can be suggested by indirect CT and MR findings, including disproportionate and severe dilatation of the bile ducts proximal or even distal to the tumor, hepatic parenchymal atrophy in the affected lobe or segments, and bulging of the papilla (Figure 10). This usually occurs in IPN-B with mucosal spreading growth without forming tangible masses, and can be explained by the production of excessive amounts of mucin and a longstanding increased ductal pressure on the adjacent hepatic parenchyma due to the partial obstruction[34].

Moreover, in our experience, mucin appears as an elongated and amorphous filling defect within an enhanced bile duct on gadobenate dimeglumine-enhanced or gadoxetic acid-enhanced MR imaging, similar to that of direct cholangiographic findings (Figure 10). The filling defect due to mucin could be confused with other intraluminal filling defects, such as a stone, blood clot, or mass. T2-weighted images can be helpful to distinguish hyperintense mucin from other intraluminal filling defects that usually appear as a signal void, or as hypointense or isointense[35].

Papillary neoplasm of the gallbladder: Mucin-producing carcinoma of the gallbladder is rare, and occurs mostly in older women. Mucin-producing carcinoma of the gallbladder histologically includes two different types: well-differentiated papillary adenocarcinoma and mucinous carcinoma. Well-differentiated adenocarcinoma (particularly papillary adenocarcinoma) usually presents as a papillary growth pattern and can produce mucin in the gallbladder lumen. A well-differentiated papillary adenocarcinoma is potentially less invasive due to its tendency toward intraluminal growth. At cross-sectional imaging, it appears as a papillary protrusion in an enlarged gallbladder[36].

Tumors composed of neoplastic epithelium containing intracellular mucin associated with little or no extracellular mucin

Signet ring cell carcinoma: Signet ring cell carcinoma is characterized by large intracytoplasmic mucin vacuoles that expand in the malignant cells and push the nucleus to the periphery, creating a "signet ring" configuration. When ⩾ 50% of the tumor is composed of cells of this type, it is classified as a signet ring cell carcinoma. More than 96% of all signet ring cell carcinomas arise in the stomach, with the rest arising in other primary organs including the rectum, colon, gallbladder, pancreas, bladder, and breast[3,4].

Signet ring cell carcinomas usually produce minimal mucosal alterations in the gastrointestinal tract, but signet

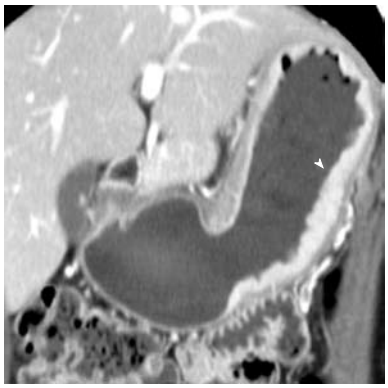

Figure 11 Signet ring cell carcinoma of the stomach in a 45-year-old woman. Coronal reformatted contrast-enhanced CT image shows diffuse gastric wall thickening with strong enhancement (arrowhead) along the lesser and greater curvature of the stomach. CT: Computed tomography.

ring cells diffusely infiltrate throughout the bowel wall and often incite a marked desmoplastic reaction in the submucosa and muscularis propria, which produces the classic pathological features of primary scirrhous carcinoma, also known as the linitis plastic type[3,4].

Gastric signet ring cell carcinoma accounts for 5%-15% of all gastric cancers, and occurs at a higher frequency in females and young patients. The prognosis of gastric signet ring cell carcinoma remains controversial. However, signet ring cell histology is generally considered a poor prognostic factor in gastric carcinoma[3]. Hyperenhancement of the involved stomach wall compared with liver attenuation on portal venous phases of contrast-enhanced CT and a predominantly thickened layer of the gastric wall are more commonly found in gastric signet ring cell carcinoma than in non-signet ring cell carcinoma (Figure 11). Hyperenhancement of the gastric lesion may correspond to intermingled loose and immature fibrosis or neovascularized signet ring cells[37].

Colorectal signet ring cell carcinoma is rare, ranging from 0.1% to 2.4% of all colorectal carcinomas. Most are localized exclusively in the rectum. This carcinoma commonly occurs in younger patients and also has a high rate of spread to the lymph nodes, ovaries, or peritoneal surface. Distant hematogenous metastasis to the liver or lung is uncommon. The most common and characteristic CT features of this tumor are a long segment of concentric wall thickening and a target appearance (Figure 12)[38]. Imaging findings of colorectal signet ring cell carcinoma are similar to those of metastatic linitis plastica originating from a primary tumor, such as breast, gastric, or bladder cancers. Metastatic linitis plastica appears as a malignant target sign consisting of thickened inner (mucosa and submucosa) and outer (serosa) layers and a relatively thin hypoattenuated middle layer (muscularis propria), or bowel wall thickening with homogeneous attenuation. In contrast, a benign target sign can be caused by submucosal edema, inflammatory infiltration, or hemorrhage and thus appears as a prominent hypoattenuating middle layer (submucosa) and thin hyperattenuating inner (mucosa) and outer layer (muscularis propria and serosa)[39].

Figure 12 Signet ring cell carcinoma of the rectum in a 42-year-old man. A, B: Axial (A) and coronal reformatted (B) contrast-enhanced CT images show concentric wall thickening with malignant target sign (arrowheads in A, arrow in B) in the rectum; C: Photomicrograph image (original magnification, × 200; HE stain) shows multiple signet ring cells. CT: Computed tomography; HE: Hematoxylin and eosin.

Tumors composed of abundant extracellular mucin due to mucin-secreting neoplastic epithelium

Mucinous adenocarcinoma of the gastrointestinal tract: Adenocarcinomas in various organs can produce and secrete extracellular mucin. This extracellular mucinous material may be so copious that the malignant cells appear to float within a gelatinous pool. Mucinous carcinoma is diagnosed when extracellular mucin within the tumor is retained by more than 50% of the cells[1,2].

Mucinous carcinoma of the gastrointestinal tract is a rare subtype of adenocarcinoma that usually occurs in the stomach and colorectum. Mucinous carcinomas in

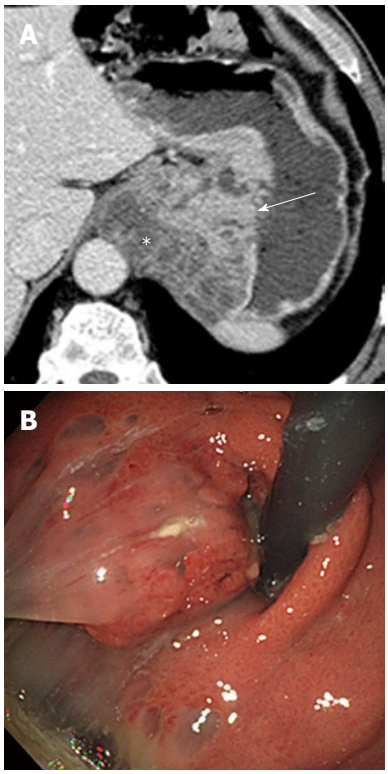

Figure 13 Mucinous carcinoma of the stomach in a 62-year-old woman. A: Contrast-enhanced CT image shows a large mass lesion in the gastric cardia containing abundant mucin pools (asterisk) and enhanced solid portions (arrow); B: Endoscopy image shows jellylike mucin leaking from the gastric mass. CT: Computed tomography.

the gastrointestinal tract have worse prognosis than non-mucinous carcinomas, because they are more frequently diagnosed in the advanced stage and are associated with deeper cancer depth, higher incidence of lymph node metastasis, lymphatic and venous permeation, and peritoneal dissemination[1,2].

Gastric mucinous carcinoma represents approximately 3% of all gastric cancers. Most gastric carcinomas are detected by endoscopy combined with biopsy. However, it is often difficult to diagnose mucinous carcinoma by biopsy because most mucinous gastric carcinomas are located predominantly in the submucosa and the frequency of mucosal involvement is somewhat low. Therefore, an accurate preoperative diagnosis of mucinous carcinomas in the gastrointestinal tract by CT or MR is important. The most common CT appearance for a gastric mucinous carcinoma is a diffuse wall thickening greater than 1 cm with preserved layering enhancement (Figure 13). A thickened hypoattenuating middle or outer layer corresponds to abundant mucin pools located in the submucosa or deeper layers, and the thin enhancing inner layer corresponds to the overlying normal mucosal layer with or without the exception of focal cancer infiltration. Miliary and punctate calcifications within the mucin pool are present and are thought to be diagnostic for mucinous adenocarcinoma[40].

Colorectal mucinous carcinoma varies from 5% to 15%

Figure 14 Mucinous adenocarcinoma of the cecum in a 69-year-old man. Contrast-enhanced CT image shows a huge eccentric hypoattenuating mass with poor enhancement of the solid portion of the cecum (asterisk). The mass has invaded the retroperitoneum (arrow). CT: Computed tomography.

of all colorectal carcinomas. Mucinous carcinoma most frequently occurs in the rectosigmoid or ascending colon. CT features indicating mucinous-type colorectal cancer include marked eccentric bowel wall thickening greater than 2 cm, heterogeneous contrast enhancement of the tumor with poor enhancement of the solid portion, a large area of hypoattenuation, and intramural calcification (Figure 14). On MR imaging, a colorectal mucinous carcinoma appears with very high signal intensity on T2-weighted images as a manifestation of the presence of extracellular mucin (Figure 15). Intratumoral congestion, abscess, necrosis and mural edema or entrapped fluids also appear with high signal intensity on T2-weighted images. A mucin tumor can be distinguished from a mimic because the tumor mucin pool may be enhanced, whereas others are not enhanced[41,42]. The enhancement pattern can be a peripheral, heterogeneous, or lacelike enhancement, corresponding to the enhancing mesh-like internal structure formed by the cells, cord, and vessels that line the pools of extracellular mucin[42].

Perianal mucinous adenocarcinoma: A perianal mucinous adenocarcinoma is a rare clinical condition that represents approximately 3% to 11% of all perianal carcinomas. Although their etiology is debatable, mucinous adenocarcinomas may originate from chronic anal fistulas, abscesses, anal glands, or intestinal duplications. This carcinoma is usually diagnosed at an advanced stage and the overall prognosis is poor[43]. CT findings suggesting a perianal mucinous adenocarcinoma include a multilocular cystic mass with peripheral calcification around the anus. It is well established that MR imaging plays an important role when evaluating a perianal mucinous carcinoma-associated fistula in ano. MR features indicating a perianal mucinous adenocarcinoma include masses filled with markedly hyperintense content on T2-weighted images, enhancing solid components, mesh-like internal enhancement, a fistula between the mass and the anus, contrast enhancement of peripheral structures or peritumoral areas, and regional areas of lymph node enlargement. A sol-

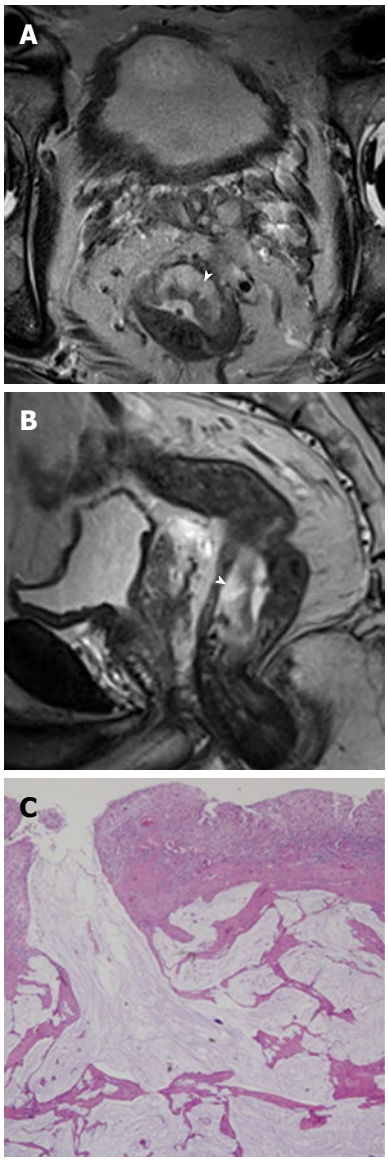

Figure 15 Mucinous adenocarcinoma of the rectum in a 63-year-old man. A, B: Axial (A) and coronal (B) T2-weighted MR images show an area of hyperintense mucin pools (arrowhead) in the rectal mass; C: Photomicrograph image (original magnification, × 40; HE stain) shows large pools of extracellular mucin and tumor cells. MR: Magnetic resonance; HE: Hematoxylin and eosin.

Figure 16 Perianal mucinous adenocarcinoma in a 41-year-old man. A: Sagittal T2-weighted MR image shows a hyperintense mass (arrowheads) in the perianal area; B: Sagittal contrast-enhanced T1-weighted MR image shows mesh-like internal enhancement (arrowheads) within the mass; C: Photomicrograph image (original magnification, × 100; HE stain) shows large pools of extracellular mucin and tumor cells. MR: Magnetic resonance; HE: Hematoxylin and eosin.

id enhancing component and mesh-like enhancement can be a clue to distinguish mucinous adenocarcinomas from abscesses associated with a fistula in ano (Figure 16)[43].

Urachal mucinous carcinoma: Urachal carcinoma is a rare neoplasm arising from the urachal remnant. Although a normal urachus is commonly lined by transitional epithelium, most urachal cancer is adenocarcinoma (90%), which is caused by metaplasia of the urachal mucosa into columnar epithelium followed by a malignant transformation. Approximately 70% of urachal carcinomas are mucinous adenocarcinomas which contain variable amounts of extracellular mucin. Although the prognosis for urachal carcinoma is slightly better than that of nonurachal adenocarcinoma, its prognosis is generally poor because this tumor arises in a clinically silent anatomical location and is generally discovered only after local invasion or metastatic disease. A characteristic CT feature of urachal carcinoma is a midline supravesical solid and partly cystic mass due to mucin produced by the tumors (Figure 17). Psammomatous calcification may occur in 50%-70% of cases. Extension of a urachal carcinoma along the Retzius space helps distinguish it from other vesical carcinomas. T2-weighted images are helpful for detecting the area of the mucin pool within the tumor[44].

Adenoma malignum: Adenoma malignum, also known as a minimal deviation adenocarcinoma, is a rare subtype of

Figure 17 Intraperitoneal spread of mucinous adenocarcinoma of the urachus (also called peritoneal mucinous carcinomatosis) in a 57-year-old man. A: Contrast-enhanced CT image shows a midline supravesical mass with heterogeneous attenuation. Within the mass are scattered low-attenuation areas (arrowheads), which represent mucin; B: Contrast-enhanced CT image of the upper abdomen shows low-attenuation mucinous ascites scalloping the liver margin. Note the right pleural effusion (asterisk) and diffuse nodular thickening of the peritoneum (arrowheads). CT: Computed tomography; MR: Magnetic resonance.

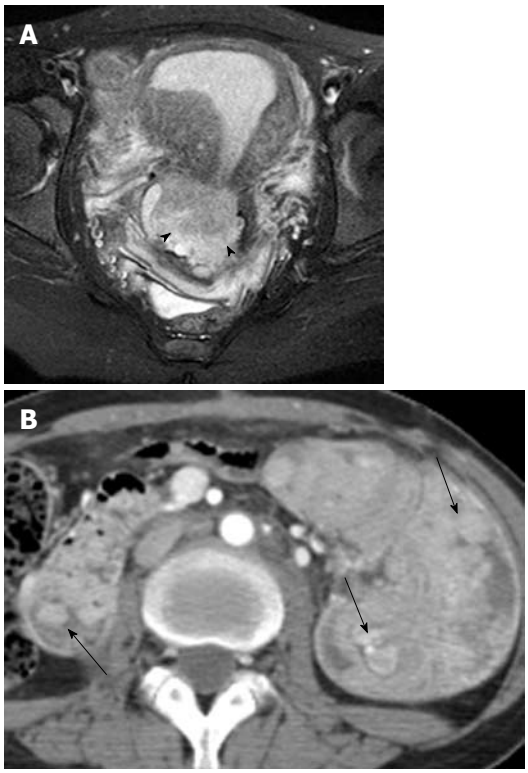

Figure 18 Adenoma malignum of the cervix in a 30-year-old woman with Peutz-Jeghers syndrome. A: Axial T2-weighted MR image shows a multicystic lesion with a solid component (arrowheads) in the uterine cervix; B: Contrast-enhanced CT image shows multiple polyps (arrows) in the duodenum and small bowel causing intussusceptions. CT: Computed tomography; MR: Magnetic resonance.

mucinous adenocarcinoma, representing about 3% of all cervical adenocarcinomas. Adenoma malignum is often associated with Peutz-Jeghers syndrome and mucinous tumors of the ovary. Despite the presence of well-differentiated histopathological features, the prognosis is unfavorable because of early dissemination into the peritoneal cavity and early distant metastasis[45].

On MR imaging, adenoma malignum is characterized by a multicystic lesion, demonstrating very high signal intensity on T2-weighted images, with some solid enhancing components in the deep cervical stroma (Figure 18). However, these MR findings are often confused with those of some other pseudoneoplastic lesions such as deep nabothian cysts, florid endocervical hyperplasia, or papillary endocervicitis, because some portions of these pseudoneoplastic cervical lesions are thickened or accompanied by solid components with enhancement, reflecting the inflammatory process in the cervix stroma or congestion of the small vessels[45].

Mucinous carcinoma of the gallbladder: Mucinous carcinoma of the gallbladder has a massive mucus pool within the carcinoma tissue, tends to growth invasively, and is associated with a poor prognosis. A mucinous carcinoma appears as a focal multilocular hypodense lesion with rim-like enhancement on contrast-enhanced CT. A hyperechoic mass on US and a near-water density on non-enhanced CT pathologically reflect a tumor containing a massive mucin pool with fibrous septa (Figure 19). Calcification within the tumor is often seen. Movable spotty and hyperechoic debris on US or movable filling defects on cholangiography inside the gallbladder lumen or biliary tree, which reflect hypersecretion of mucin, are helpful for diagnosing a mucin-producing carcinoma of the gallbladder. Dilatation of the cystic duct, intrahepatic ducts, or common bile duct is sometimes seen[36].

Mucinous type of cholangiocarcinoma: Mucinous carcinoma is the rarest histological type of cholangiocarcinoma. Mucinous carcinoma appears as an extremely hypodense mass with marginal or septal enhancement on contrast-enhanced CT, and as an extremely hypointense and hyperintense mass on T1- and T2-weighted images, respectively. Its radiological characteristics reflect large mucinous lakes throughout the tumor without mucin excretion into the bile duct[46].

PSEUDOMYXOMA PERITONEI

PMP is an uncommon clinical condition characterized by

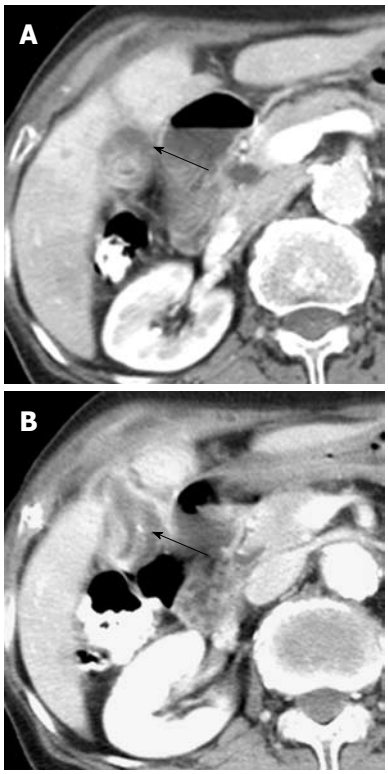

Figure 19 Mucinous carcinoma of the gallbladder in a 77-year-old woman. A: Contrast-enhanced CT image shows localized wall thickening (arrow) in the body of the gallbladder containing a suspicious mucin pool; B: Contrast-enhanced CT image inferior to (A) shows a punctate calcification and localized wall thickening (arrow) in a mildly distended gallbladder. CT: Computed tomography.

accumulation of copious gelatinous materials throughout the peritoneal cavity. It is found in one of 5000 laparotomies, and occurs more commonly in women than men. PMP occurs when mucin-producing lesions rupture into the peritoneal cavity. PMP due to rupture of an appendiceal mucocele is the most common. Mucinous tumors arising from the ovary, gastrointestinal tract, pancreas, and urachus may also cause PMP. However, its origin may not be clear due to extensive organ involvement. Coexistence of mucinous tumors of the appendix and ovary are frequently observed in most women with PMP (Figure 4). Although relationship of PMP to other tumors continues to be controversial, ovarian tumors may represent a secondary deposit from appendiceal tumors[47]. Although most pseudomyxomas are in the peritoneal cavity, they may occur in the retroperitoneum. Pseudomyxoma retroperitonei is caused by rupture of a retrocecal appendiceal mucocele into the retroperitoneal space and fixation of the lesion to the posterior abdominal wall[48].

PMP may be classified into three clinicopathological categories: disseminated peritoneal adenomucinosis (DPAM), peritoneal mucinous carcinomatosis (PMCA), and PMCA with features intermediate between DPAM and PMCA or with discordant features. DPAM is characterized by peritoneal lesions composed of abundant extracellular mucin containing scant mucinous epithelium with little cytologic atypia or mitotic activity, whereas PMCA is characterized by peritoneal lesions composed of more abundant mucinous epithelium with the architectural and cytologic features of carcinoma. Because DPAM is histologically benign, its prognosis is better than that of PMCA[49].

On CT, PMP appears as ascites with attenuation slightly higher than water. It initially accumulates at sites of relative stasis such as the pouch of Douglas/rectovesical pouch, the right and left subphrenic space, or the surface of the liver and spleen. Septa, curvilinear or amorphous calcification, areas of soft tissue attenuation due to solid elements within mucinous material, or compressed mesentery are seen more commonly within PMP as the volume of disease increases. Scalloping of the visceral surface, particularly the liver, is the diagnostic feature that distinguishes mucinous from simple ascites (Figures 4, 8 and 17). Although CT findings of DPAM and PMCA overlap considerably, PMCA tends to be more frequently accompanied by coexistent pleural masses or effusion, lymphadenopathy, and diffuse peritoneal infiltration such as omental cakes (Figure 17)[49].

CONCLUSION

Various mucin-producing neoplasms originate in different abdominal and pelvic organs. Distinguishing mucinous from non-mucinous tumors is important because of the differences in clinical outcome. Imaging modalities play a critical role in differentiating these two entities. Due to high water content, mucin has a similar appearance to water on both CT and MR imaging, except when thick and proteinaceous, and then it tends to be hyperdense compared to water and hyperintense on T1- and hypointense on T2-weighted images. A correct diagnosis of mucin-producing neoplasms is possible when these imaging features are identified on cross-sectional imaging. Because imaging features of mucin can have a similar appearance to water in both CT and MR imaging, the differentiation of mucinous from non-mucinous neoplastic conditions *via* only imaging features of mucin is sometimes problematic. In addition, further studies with appropriate quantitative and statistical analyses are required to confirm whether these imaging findings can be helpful in the correct diagnosis of mucin-producing neoplasms. However, the imaging appearance of mucin-producing neoplasms differs somewhat depending on the organ of origin; additional information about the distinctive imaging features of mucin-producing neoplasms according to tumor location may also facilitate accurate diagnosis and treatment.

REFERENCES

1 **Zhang M**, Zhu GY, Zhang HF, Gao HY, Han XF, Xue YW. Clinicopathologic characteristics and prognosis of mucinous gastric carcinoma. *J Surg Oncol* 2010; **102**: 64-67
2 **Consorti F**, Lorenzotti A, Midiri G, Di Paola M. Prognostic significance of mucinous carcinoma of colon and rectum: a

prospective case-control study. *J Surg Oncol* 2000; **73**: 70-74
3 **Maehara Y**, Sakaguchi Y, Moriguchi S, Orita H, Korenaga D, Kohnoe S, Sugimachi K. Signet ring cell carcinoma of the stomach. *Cancer* 1992; **69**: 1645-1650
4 **Tung SY**, Wu CS, Chen PC. Primary signet ring cell carcinoma of colorectum: an age- and sex-matched controlled study. *Am J Gastroenterol* 1996; **91**: 2195-2199
5 **Lim JH**, Lee G, Oh YL. Radiologic spectrum of intraductal papillary mucinous tumor of the pancreas. *Radiographics* 2001; **21**: 323-337; discussion 337-340
6 **Lim JH**, Yoon KH, Kim SH, Kim HY, Lim HK, Song SY, Nam KJ. Intraductal papillary mucinous tumor of the bile ducts. *Radiographics* 2004; **24**: 53-66; discussion 66-67
7 **Allen A**, Flemström G, Garner A, Kivilaakso E. Gastroduodenal mucosal protection. *Physiol Rev* 1993; **73**: 823-857
8 **Corfield AP**, Carroll D, Myerscough N, Probert CS. Mucins in the gastrointestinal tract in health and disease. *Front Biosci* 2001; **6**: D1321-D1357
9 **Hollingsworth MA**, Swanson BJ. Mucins in cancer: protection and control of the cell surface. *Nat Rev Cancer* 2004; **4**: 45-60
10 **Gaeta M**, Vinci S, Minutoli F, Mazziotti S, Ascenti G, Salamone I, Lamberto S, Blandino A. CT and MRI findings of mucin-containing tumors and pseudotumors of the thorax: pictorial review. *Eur Radiol* 2002; **12**: 181-189
11 **Buetow PC**, Rao P, Thompson LD. From the Archives of the AFIP. Mucinous cystic neoplasms of the pancreas: radiologic-pathologic correlation. *Radiographics* 1998; **18**: 433-449
12 **Sahani DV,** Kadavigere R, Saokar A, Fernandez-del Castillo C, Brugge WR, Hahn PF. Cystic pancreatic lesions: a simple imaging-based classification system for guiding management. *Radiographics* 2005; **25**: 1471-1484
13 **Morel A**, Marteau V, Chambon E, Gayet B, Zins M. Pancreatic mucinous cystadenoma communicating with the main pancreatic duct on MRI. *Br J Radiol* 2009; **82**: e243-e245
14 **Kalb B**, Sarmiento JM, Kooby DA, Adsay NV, Martin DR. MR imaging of cystic lesions of the pancreas. *Radiographics* 2009; **29**: 1749-1765
15 **Buetow PC**, Buck JL, Pantongrag-Brown L, Ros PR, Devaney K, Goodman ZD, Cruess DF. Biliary cystadenoma and cystadenocarcinoma: clinical-imaging-pathologic correlations with emphasis on the importance of ovarian stroma. *Radiology* 1995; **196**: 805-810
16 **Lewin M**, Mourra N, Honigman I, Fléjou JF, Parc R, Arrivé L, Tubiana JM. Assessment of MRI and MRCP in diagnosis of biliary cystadenoma and cystadenocarcinoma. *Eur Radiol* 2006; **16**: 407-413
17 **Palacios E**, Shannon M, Solomon C, Guzman M. Biliary cystadenoma: ultrasound, CT, and MRI. *Gastrointest Radiol* 1990; **15**: 313-316
18 **Lim JH**, Jang KT, Rhim H, Kim YS, Lee KT, Choi SH. Biliary cystic intraductal papillary mucinous tumor and cystadenoma/cystadenocarcinoma: differentiation by CT. *Abdom Imaging* 2007; **32**: 644-651
19 **Hart WR**. Mucinous tumors of the ovary: a review. *Int J Gynecol Pathol* 2005; **24**: 4-25
20 **Imaoka I**, Wada A, Kaji Y, Hayashi T, Hayashi M, Matsuo M, Sugimura K. Developing an MR imaging strategy for diagnosis of ovarian masses. *Radiographics* 2006; **26**: 1431-1448
21 **Bazot M**, Daraï E, Nassar-Slaba J, Lafont C, Thomassin-Naggara I. Value of magnetic resonance imaging for the diagnosis of ovarian tumors: a review. *J Comput Assist Tomogr* 2008; **32**: 712-723
22 **Okamoto Y**, Tanaka YO, Tsunoda H, Yoshikawa H, Minami M. Malignant or borderline mucinous cystic neoplasms have a larger number of loculi than mucinous cystadenoma: a retrospective study with MR. *J Magn Reson Imaging* 2007; **26**: 94-99
23 **Bent CL**, Sahdev A, Rockall AG, Singh N, Sohaib SA, Reznek RH. MRI appearances of borderline ovarian tumours. *Clin Radiol* 2009; **64**: 430-438
24 **Pickhardt PJ**, Levy AD, Rohrmann CA, Kende AI. Primary neoplasms of the appendix: radiologic spectrum of disease with pathologic correlation. *Radiographics* 2003; **23**: 645-662
25 **Honnef I**, Moschopulos M, Roeren T. Appendiceal mucinous cystadenoma. *Radiographics* 2008; **28**: 1524-1527
26 **Caspi B**, Cassif E, Auslender R, Herman A, Hagay Z, Appelman Z. The onion skin sign: a specific sonographic marker of appendiceal mucocele. *J Ultrasound Med* 2004; **23**: 117-121; quiz 122-123
27 **Lim HK**, Lee WJ, Kim SH, Kim B, Cho JM, Byun JY. Primary mucinous cystadenocarcinoma of the appendix: CT findings. *AJR Am J Roentgenol* 1999; **173**: 1071-1074
28 **Bennett GL**, Tanpitukpongse TP, Macari M, Cho KC, Babb JS. CT diagnosis of mucocele of the appendix in patients with acute appendicitis. *AJR Am J Roentgenol* 2009; **192**: W103-W110
29 **Paal E**, Thompson LD, Przygodzki RM, Bratthauer GL, Heffess CS. A clinicopathologic and immunohistochemical study of 22 intraductal papillary mucinous neoplasms of the pancreas, with a review of the literature. *Mod Pathol* 1999; **12**: 518-528
30 **Nakanuma Y**. A novel approach to biliary tract pathology based on similarities to pancreatic counterparts: is the biliary tract an incomplete pancreas? *Pathol Int* 2010; **60**: 419-429
31 **Lim JH**, Jang KT. Mucin-producing bile duct tumors: radiological-pathological correlation and diagnostic strategy. *J Hepatobiliary Pancreat Sci* 2010; **17**: 223-229
32 **Kim H**, Lim JH, Jang KT, Kim MJ, Lee J, Lee JY, Choi D, Lim HK, Choi DW, Lee JK, Baron R. Morphology of intraductal papillary neoplasm of the bile ducts: radiologic-pathologic correlation. *Abdom Imaging* 2011; **36**: 438-446
33 **Chung YE**, Kim MJ, Park YN, Choi JY, Pyo JY, Kim YC, Cho HJ, Kim KA, Choi SY. Varying appearances of cholangiocarcinoma: radiologic-pathologic correlation. *Radiographics* 2009; **29**: 683-700
34 **Lim JH**, Jang KT, Choi D. Biliary intraductal papillary-mucinous neoplasm manifesting only as dilatation of the hepatic lobar or segmental bile ducts: imaging features in six patients. *AJR Am J Roentgenol* 2008; **191**: 778-782
35 **Park MS**, Yu JS, Lee DK, Yoon DS, Cha SW, Kim KW. Gadobenate dimeglumine-enhanced MRI of intraductal papillary mucinous tumor of the bile ducts. *J Magn Reson Imaging* 2007; **25**: 625-627
36 **Tian H**, Matsumoto S, Takaki H, Kiyosue H, Komatsu E, Okino Y, Mori H, Miyake H. Mucin-producing carcinoma of the gallbladder: imaging demonstration in four cases. *J Comput Assist Tomogr* 2003; **27**: 150-154
37 **Lee JH**, Park MS, Kim KW, Yu JS, Kim MJ, Yang SW, Lee YC. Advanced gastric carcinoma with signet ring cell carcinoma versus non-signet ring cell carcinoma: differentiation with multidetector CT. *J Comput Assist Tomogr* 2006; **30**: 880-884
38 **Kim HJ**, Ha HK, Cho KS, Yu E, Kim JC, Yoo CS, Kim HC, Yang SK, Jeong HY, Auh YH. CT features of primary colorectal signet-ring cell carcinoma. *J Comput Assist Tomogr* 2001; **25**: 225-230
39 **Gollub MJ**, Schwartz MB, Shia J. Scirrhous metastases to the gastrointestinal tract at CT: the malignant target sign. *AJR Am J Roentgenol* 2009; **192**: 936-940
40 **Park MS**, Yu JS, Kim MJ, Yoon SW, Kim SH, Noh TW, Lee KH, Lee JT, Yoo HS, Kim KW. Mucinous versus nonmucinous gastric carcinoma: differentiation with helical CT. *Radiology* 2002; **223**: 540-546
41 **Ko EY**, Ha HK, Kim AY, Yoon KH, Yoo CS, Kim HC, Kim JC. CT differentiation of mucinous and nonmucinous colorectal carcinoma. *AJR Am J Roentgenol* 2007; **188**: 785-791
42 **Kim MJ**, Park JS, Park SI, Kim NK, Kim JH, Moon HJ, Park

YN, Kim WH. Accuracy in differentiation of mucinous and nonmucinous rectal carcinoma on MR imaging. *J Comput Assist Tomogr* 2003; **27**: 48-55

43 **Hama Y**, Makita K, Yamana T, Dodanuki K. Mucinous adenocarcinoma arising from fistula in ano: MRI findings. *AJR Am J Roentgenol* 2006; **187**: 517-521

44 **Koster IM**, Cleyndert P, Giard RW. Best cases from the AFIP: urachal carcinoma. *Radiographics* 2009; **29**: 939-942

45 **Okamoto Y**, Tanaka YO, Nishida M, Tsunoda H, Yoshikawa H, Itai Y. MR imaging of the uterine cervix: imaging-pathologic correlation. *Radiographics* 2003; **23**: 425-445; quiz 534-535

46 **Hayashi M**, Matsui O, Ueda K, Kadoya M, Yoshikawa J, Gabata T, Takashima T, Izumi R, Nakanuma Y. Imaging findings of mucinous type of cholangiocellular carcinoma. *J Comput Assist Tomogr* 1996; **20**: 386-389

47 **Ronnett BM**, Kurman RJ, Zahn CM, Shmookler BM, Jablonski KA, Kass ME, Sugarbaker PH. Pseudomyxoma peritonei in women: a clinicopathologic analysis of 30 cases with emphasis on site of origin, prognosis, and relationship to ovarian mucinous tumors of low malignant potential. *Hum Pathol* 1995; **26**: 509-524

48 **Matsuoka Y**, Masumoto T, Suzuki K, Terada K, Ushimi T, Yokoyama Y, Abe K, Kamata N, Yasuno M, Hishima T. Pseudomyxoma retroperitonei. *Eur Radiol* 1999; **9**: 457-459

49 **Bechtold RE**, Chen MY, Loggie BW, Jackson SL, Geisinger K. CT appearance of disseminated peritoneal adenomucinosis. *Abdom Imaging* 2001; **26**: 406-410

S- Editor Sun H **L- Editor** Logan S **E- Editor** Zhang DN